

GLUCOSE OXIDASE IMMOBILIZATION ONTO CARBON NANOTUBE NETWORKING

V.A. KARACHEVTSEV,¹ A.YU. GLAMAZDA,¹ E.S. ZARUDNEV,¹
M.V. KARACHEVTSEV,¹ V.S. LEONTIEV,¹ A.S. LINNIK,¹ O.S. LYTVYN,²
A.M. PLOKHOTNICHENKO,¹ S.G. STEPANIAN¹

¹**B. Verkin Institute for Low Temperature Physics and Engineering,
Nat. Acad. of Sci. of Ukraine**
(47, Lenin Ave., Kharkov 61103, Ukraine)

²**V. Lashkaryov Institute of Semiconductor Physics, Nat. Acad. of Sci. of Ukraine**
(41 Nayki Ave., 03028 Kyiv, Ukraine)

PACS 78.67.Ch
©2012

When elaborating the biosensor based on single-walled carbon nanotubes (SWNTs), it is necessary to solve such an important problem as the immobilization of a target biomolecule on the nanotube surface. In this work, the enzyme (glucose oxidase (GOX)) was immobilized on the surface of a nanotube network, which was created by the deposition of nanotubes from their solution in 1,2-dichlorobenzene by the spray method. 1-Pyrenebutanoic acid succinimide ester (PSE) was used to form the molecular interface, the bifunctional molecule of which provides the covalent binding with the enzyme shell, and its other part (pyrene) is adsorbed onto the nanotube surface. First, the usage of such a molecular interface leaves out the direct adsorption of the enzyme (in this case, its activity decreases) onto the nanotube surface, and, second, it ensures the enzyme localization near the nanotube. The comparison of the resonance Raman (RR) spectrum of pristine nanotubes with their spectrum in the PSE environment evidences the creation of a nanohybrid formed by an SWNT with a PSE molecule which provides the further enzyme immobilization. As the RR spectrum of an SWNT:PSE:GOX film does not essentially differ from that of SWNT:PSE ones, this indicates that the molecular interface (PSE) isolates the enzyme from nanotubes strongly enough. The efficient immobilization of GOX along the carbon nanotubes due to PSE is confirmed with atom-force microscopy images. The method of molecular dynamics allowed us to establish the structures of SWNT:PSE:GOX created in the aqueous environment and to determine the interaction energy between hybrid components. In addition, the conductivity of the SWNT network with adsorbed PSE and GOX molecules is studied. The adsorption of PSE molecules onto the SWNT network causes a decrease of the conductivity, which can be explained by the appearance of scattering centers for charge carriers on the nanotube surface, which are created by PSE molecules.

applications including the biosensing. The main challenge in the development of the devices is the biofunctionalization of nanomaterial surfaces and the creation of appropriate interfaces between the nanotubes and the biosystems. Carbon-nanotube-based biological sensors could find applications, for example, in measuring the concentrations of glucose in blood. This is particularly important because the number of diabetics in the world increases continuously and dramatically.

In the last few years, the applications of conducting properties of carbon nanotubes in the biological sensing have demonstrated the high efficiency of this approach, despite the elaborations being in their infancy [1–3]. The use of the conductivity of carbon nanotubes as the detection and measuring method in midget biosensors showed some preferences over the optical methods currently being employed in the clinical work. This is related to the fact that the most of biological processes involve electrostatic interactions and/or a charge transfer, which can be directly detected with the electronic equipment. Carbon nanotubes can be easily integrated into the electronic device. Moreover, the average size of a nanotube is usually compatible with the molecular size of a compound being analyzed, which increases the sensitivity of the measurement. The conductivities of individual nanotubes or carbon nanotube networks can be utilized in the investigation and the development of biosensors [4, 5]. Networks formed by hundreds or thousands of carbon nanotubes distributed randomly between metallic contacts have a larger active area for the detection and can operate at higher currents. The technology for the fabrication of carbon-nanotube networks is well developed and does not require the expensive equipment to operate. The networks can be produced from solutions by deposition onto various substrates.

1. Introduction

Due to their unusual physical, optical, thermal, and electronic properties, single-walled carbon nanotubes (SWNTs) have a huge potential of different promising

When working out biological sensors, in which an SWNT network is used, it is necessary to solve such an important problem as the immobilization of a recognition biomolecule on the nanotube surface. In researches, an enzyme immobilized on a nanotube is often used as the recognition element. In some works, the enzyme was immobilized directly onto the nanotube surface [6]. However, the recent work [7] showed that the activity of two enzymes (R-chymotrypsin and soybean peroxidase) decreased significantly after their adsorption onto the surface of single-walled carbon nanotubes. Thus, the problem of enzyme immobilization on a nanotube that needs to be solved is to retain the enzyme native activity despite its immobilization on the nanotube surface. The problem is closely related to the nanotube functionalization. Some success on this front has been achieved owing to the use of a molecular anchor [8, 9] or the polymer-wrapping of nanotubes [6]. The efficient non-covalent carbon nanotube functionalization by organic molecules for the biocompatibility testing was suggested by Chen and co-workers [8]. Their approach utilizes a bifunctional molecule containing succinimidyl ester and a pyrene moiety to bind proteins to the nanotube surface. Pyrene attaches to the nanotube surface by means of the $\pi-\pi$ stacking and the hydrophobic interaction and does not disrupt the nanotube backbone. Another fragment of the anchor molecule is succinimidyl ester that binds enzymes to the nanotube surface. This molecular interlayer provides a sufficiently strong attachment of the enzyme to the nanotube surface and leaves the enzyme activity unaffected. The enzyme localization near the nanotube needs to provide the reliable detection of the charge, which appears as a result of the biochemical reaction of enzymes with the probe.

In the present work, the enzyme (glucose oxidase (GOX)) was immobilized onto the surface of a nanotube network, which was created by the deposition of nanotubes from their solution in dichlorobenzene by the spray method. 1-pyrenebutanoic acid N-hydroxysuccinimide ester (PSE) was used to form the molecular interface. The comparison of the resonance Raman (RR) light scattering spectrum of pristine nanotubes with their spectrum in the PSE environment evidences the creation of a nanohybrid formed by SWNT with a PSE molecule which ensures the further enzyme immobilization. As the RR spectrum of an SWNT:PSE:GOX film does not essentially differ from that of SWNT:PSE ones, this indicates that the molecular interface (PSE) isolates the enzyme from nanotubes efficiently. The immobilization of GOX near a carbon nanotube due to PSE is confirmed by atom-force microscopy (AFM). The method

of molecular dynamics allows us to establish the structures of SWNT:PSE:GOX and to determine the energies of the intermolecular interaction between components of the triple complex in the aqueous environment. In addition, we study the conductivity of the SWNT network with adsorbed PSE and GOX molecules. The adsorption of PSE molecules on the SWNT network results in a decrease of the conductivity, which is most likely induced by the appearance of scattering centers for charge carriers in nanotubes.

2. Experimental

SWNTs have been produced by the CoMoCAT method (SouthWest NanoTechnologies Inc., USA). This method yields nanotubes with narrow diameters (0.75–0.95 nm) and chirality (6,5) [10]. PSE was purchased from Sigma-Aldrich, Europe. All compounds have been used without additional purification.

Nanotube suspensions were prepared in dichlorobenzene (Sigma-Aldrich, Europe), which is the most efficient organic solvent for nanotubes. Suspensions were obtained by ultrasonication (44 kHz, UZDN-2, Sumy, Ukraine) and by the following ultracentrifugation (up to 18 000 g). As a result, all insoluble thick bundles of nanotubes, as well as the metallic catalyst, were precipitated. To get one sample, we used 0.2 mg of nanotubes, being dissolved in 4 ml of dichlorobenzene.

The carbon nanotube network on the substrate (quartz) was created by the spray method. To form this network, a special electronic device was constructed to control the nanotube network density, by using the conductivity of the deposited network and a quartz microbalance. This density was regulated by the variation of the deposition time, as well as with the nanotube concentration in a solution. After the drying of such a nanotube network, two gold contact areas with 10 μm gap between them were thermodeposited. Glucose oxidase (GOX) was immobilized onto the carbon nanotube network through PSE, which formed a molecular interface between nanotubes and the enzyme [8]. PSE was adsorbed from its solution in methanol (10^{-4} M), and then GOX from its solution in water (10^{-4} M) was deposited.

The GOX immobilization onto carbon nanotubes was controlled with an AFM Nanoscope D3000 (Digital Instruments, USA), as well as with RR spectroscopy. For AFM measurements, nanotubes were sprayed on mica. For Raman measurements, three dried films were prepared: pristine nanotubes, nanotubes with PSE, and SWNT:PSE:GOX. To prepare the film of nanotubes with adsorbed PSE molecules, SWNTs were mixed with PSE

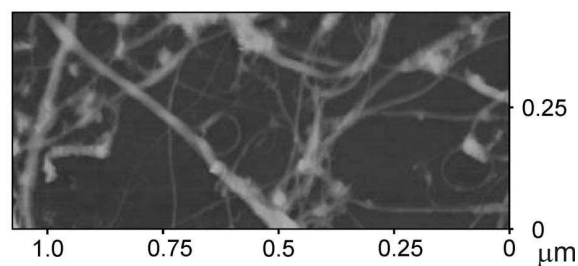


Fig. 1. AFM image of the carbon nanotube network on a mica substrate obtained by the spray method from an SWNT solution in dichlorobenzene

in methanol (with 1:1 weight ratio, 0.3 mg/ml). The mixture was treated with the sonication (1 W, 44 kHz) for 30 min. Then the suspension was deposited on the quartz substrate and dried under a stream of warm air. SWNT:PSE:GOX hybrids were prepared by the adsorption of GOX from an aqueous solution on an SWNT:PSE film. Raman experiments have been performed in the 90° scattering configuration relative to the laser beam, by using 632.8 nm (1.96 eV) light from a He-Ne laser. The spectra were analyzed using a Raman double monochromator with the reverse dispersion of $3\text{\AA}/\text{mm}$ and were detected with a thermocooled CCD camera. The position of peaks of the bands in the RR spectrum of a nanotube film was determined with the accuracy not worse than 0.3 cm^{-1} . This level of accuracy has been achieved due to the observation of the plasma lines of a laser in the spectra in a vicinity of the bands corresponding to the tangential mode (G) and the radial breathing mode (RBM) of nanotubes, which were used in the internal calibration of a spectrometer.

Volt-ampere characteristics of the nanotube network were determined by the home-built set-up based on a microcontroller, by means of which the required range of voltages was formed. A microamperemeter, which measured a current through the network, was connected with a computer. A minimal step of the output voltage was 2 mV, and the current sensitivity reached 0.1 nA.

SWNT hybrids with PSE and with GOX were modeled by the molecular dynamics method employing NAMD programs [11]. In these calculations, the force field Charmm27 was used [12]. For the enzyme, the standard force parameters were applied, and the force parameters of aromatic carbon were given to carbon nanotube atoms. Glucose oxidase was obtained from the Protein Data Bank. Its structure parameters were determined earlier [13]. A PSE molecule has no standard parameters in this force field. Therefore, an additional calculation within the DFT method was made (PSE parametriza-

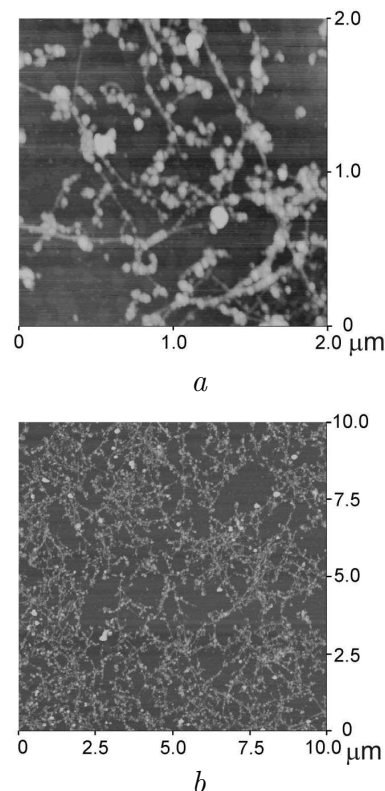


Fig. 2. AFM image of SWNT:PSE:GOX hybrids on a mica substrate

tion is described in details in [14]). In this work, carbon nanotubes 7.95 \AA in diameter, 95.2 \AA in length, and with chirality (10,0) were used. Each system was placed in a cubic water box. The distance between the hybrid under study and walls of the water box was not less than 12 \AA . Upon modeling, periodic conditions were used. Upon modeling the pressure (1 bar), the temperature (293 °K) and the atom number in the system were unchanged. At the modeling beginning, the energy of the system was minimized during 1000 cycles. The VMD Program was applied for the visualization of the results of calculations [15].

3. Results and Discussion

3.1. Analysis of the enzyme immobilization onto SWNTs by AFM

We used the AFM method to study the morphology of the network of SWNT deposited onto mica from a solution of nanotubes in dichlorobenzene. Figure 1 shows the network of SWNTs obtained by the spray method on mica. Both single nanotubes and their bundles can

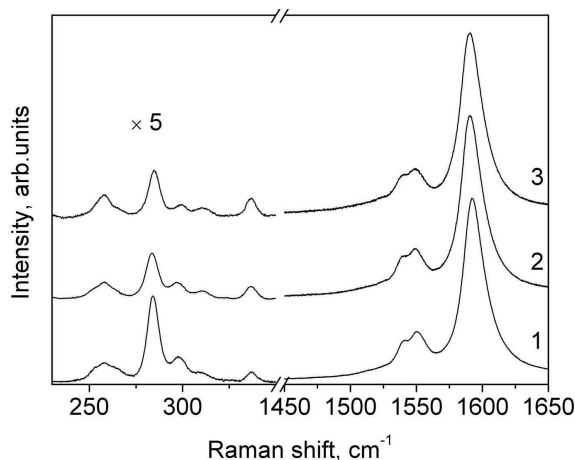


Fig. 3. Raman spectra of SWNTs (1), SWNT:PSE (2) SWNT:PSE:GOX (3) hybrids in the range of the RBM and G modes. Each experimental spectrum obtained by the laser excitation at $\lambda_{\text{exc}} = 632.8$ nm

be seen in Fig. 1. Then we deposited the molecular interface (PSE) on the network, and finally the enzyme GOX was immobilized. The AFM image of these hybrids is presented in Fig. 2. As is seen from Fig. 2, the GOX globular structures are mainly placed along nanotubes, and their heights are in the 4.38–6.37-nm range. As the height of one enzyme globule is about 4 nm [6], the obtained heights are the sum of heights of a COX globule and a nanotube. The surface of some nanotubes is fully covered with the enzyme. The detailed analysis of hybrid heights revealed that they may be 8–8.5 nm in some cases, and this indicates that the enzyme dimer is created on a nanotube. Thus, it may be concluded that, due to the PSE molecular interface, the enzyme is placed near the nanotube surface.

3.2. Raman spectroscopy of carbon nanotubes in the PSE and GOX environments

Information on the noncovalent interactions of organic molecules with the nanotube surface can be obtained from the analysis of the RR spectra of carbon nanotubes before and after the deposition of these molecules [16]. The noncovalent interaction of a nanotube and an organic molecule results in a shift of the nanotube vibrational modes and in the intensity redistribution between bands. At first, we studied such spectra of pristine nanotubes in bundles. Then we measured the spectra of nanotubes with deposited PSE molecules and, finally, after the immobilization of GOX molecules. Figure 3 presents the RR spectra of a nanotube network in the 225–1650 cm^{-1} range before (1) and after (2) the de-

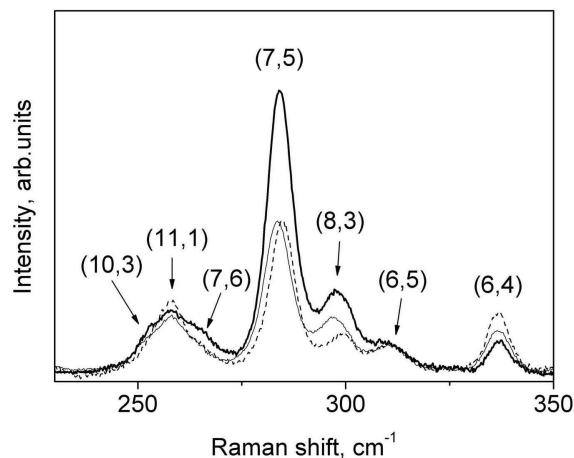


Fig. 4. Low-frequency fragment of the spectra of SWNTs (bold line), SWNT:PSE (thin line), and SWNT:PSE:GOX (broken line) in the RBM range

position of PSE, as well as after the addition of GOX (3). It should be noted that the spectra are similar, but the detailed analysis of some bands reveals some slight change in the spectrum after the PSE deposition onto the nanotube surface.

To analyze these changes in more details, we studied the most informative fragments of the RR spectra of nanotubes: ranges of the RBM (225–350 cm^{-1}) and G (1500–1650 cm^{-1}) modes.

3.2.1 Radial breathing mode

Figure 4 presents the low-frequency fragment of the RR spectrum of nanotubes, in which the RBM is observed. At the excitation by a He–Ne laser in the 225–350 cm^{-1} range, seven intense bands are observed for nanotubes obtained by the CoMoCat method. The spectra were approximated with a sum of seven Lorentzians. The frequency position of the peaks, area, and width at the half of the height of bands for the both samples were determined. These results are presented in Table 1. The nanotube chirality shown in Table 1 was determined earlier for these nanotubes [17]. As follows from Table 1, all bands were assigned to semiconducting nanotubes. The spectra were normalized to the intensity of the high-frequency component of the G-mode (G^+), which allowed us to compare the band intensities in the spectra of three samples.

As follows from Table 1, the spectral shift in the RBM (~ 1.4 cm^{-1}) is observed for SWNT:PSE in comparison with SWNT bundles. This shift is caused by the interaction of PSE molecules with nanotubes. In addition, a decrease and an enhancement of the band inten-

Table 1. Position (ω_{RBM} , cm^{-1}), width at the half of the height ($\Delta\Gamma$, cm^{-1}), integral intensity of Lorentzian curves normalized to the band corresponding to the G^+ band, chirality of nanotubes (n,m), and second electronic transition of the semiconducting SWNTs (E_{22}^S , eV) located close to the excitation energy of a He–Ne laser (1.96 eV)

(n,m)	E_{22}^S , eV [17]	SWNT			SWNT:PSE			SWNT:PSE:GOX		
		ω , cm^{-1}	$\Delta\Gamma$, cm^{-1}	S/S_G^+ $\times 100\%$	ω , cm^{-1}	$\Delta\Gamma$, cm^{-1}	S/S_G^+ $\times 100\%$	ω , cm^{-1}	$\Delta\Gamma$, cm^{-1}	S/S_G^+ $\times 100\%$
10.3	1.90	252.4	7.4	0.24	251.4	7.2	0.25	252.4	5.8	0.12
11.1	2.00	257.9	8.6	0.56	257.9	7.0	0.40	257.9	7.4	0.59
7.6	1.90	265.5	7.4	0.37	264.1	6.9	0.22	265.8	7.1	0.19
7.5	1.88	284.2	7.1	2.49	283.6	7.2	1.36	284.7	6.7	1.22
8.3	1.87	298.1	9.6	1.23	297.3	9.4	0.59	299.2	8.8	0.36
6.5	2.18	310.7	7.2	0.26	310.8	8.3	0.21	311.0	6.9	0.19
6.4	2.09	337.2	4.9	0.21	336.7	5.2	0.29	336.6	4.7	0.37

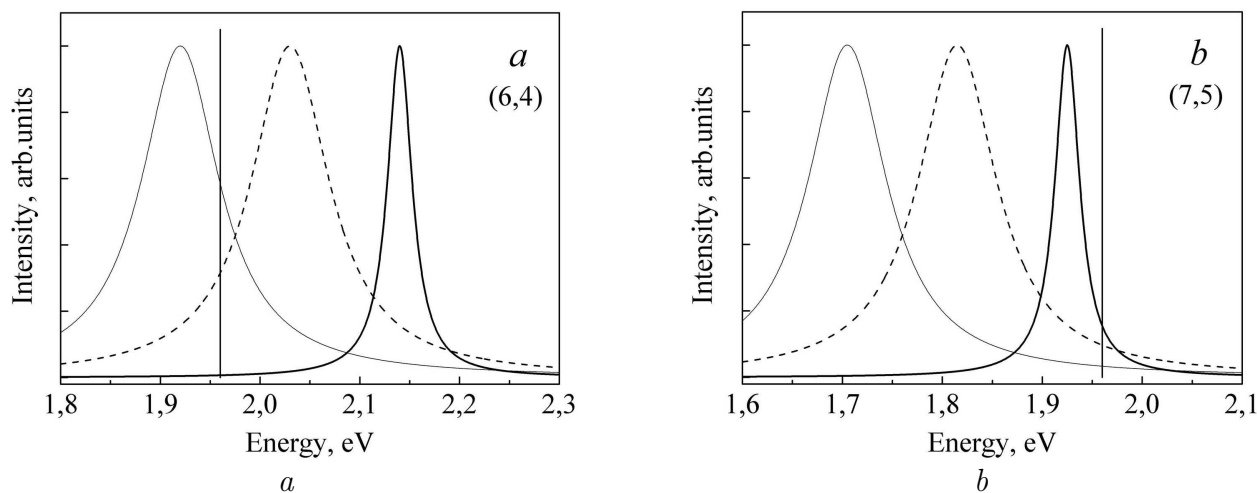


Fig. 5. Scheme of the resonant windows of semiconducting nanotubes with different chiralities (6,4) (a) and (7,5) (b) in the SDS surrounding (solid curve), SWNTs in the film (thin line) and SWNT:PSE (broken line). The energy (1.96 eV) of a He–Ne laser is shown by the vertical line. Lorentzian curves were used to describe the contours of resonant windows

sities are seen at 265.5, 284.2, 298.1 cm^{-1} and at 257.9, 310.7, 337.2 cm^{-1} , respectively. It is known that the RBM bands are very sensitive to resonance conditions, which are determined by the location of the nanotube electronic level relative to the laser energy. It is well known that the position of the nanotube electronic level depends on the interaction with the environment [18]. Thus, when the nanotube electronic level (in our case, it is the second electronic level (E_{22}^S)) is located higher than the energy of a laser, it becomes lower upon the environmental interaction, the resonance conditions are improved, and the intensity of the corresponding band increases. Otherwise, the resonance conditions become worse, and the intensity of the corresponding band decreases.

The resonance windows for two semiconducting nanotubes with different positions of electronic levels relatively to the laser energy (1.96 eV) are schematically

shown in Fig. 5. The laser energy is marked with the vertical line. Other lines are obtained using Lorentz functions. In addition, the bands corresponding to the aqueous suspension of nanotubes with a surfactant (sodium dodecyl sulfate (SDS)) (thick line) and in the film (thin line) and their hybrids with PSE (thin broken line) are shown in Fig. 5. The energy of the electronic transition for nanotubes (E_{22}^S) in the aqueous suspension of individual nanotubes with the SDS is by 60–160 meV higher, than the energy of this level for nanotubes in a film [18, 19]. This red shift is due to the strong interaction of nanotubes in bundles, which are situated in a film. For SWNT:PSE, the bundling effect is much smaller, because the organic molecules become embedded between nanotubes in bundles in a solution during the ultrasonication and, thus, decrease the interaction of nanotubes. As a result, due to the interaction between nanotubes and organic molecules, the E_{22}^S level for such

SWNTs is still lower than that for individual nanotubes in an aqueous suspension.

In our case, the nanotubes with (11,1), (6,5), and (6,4) chiralities have the electronic level (E_{22}^S), which is higher than the laser energy. So, under the interaction of nanotubes with PSE, the band intensity increases. This rule works unambiguously for nanotubes with (6,4) chirality. Contrary to this, the level E_{22}^S of nanotubes with (10,3), (7,6), (7,5), and (8,3) chiralities is lower than the laser energy. Therefore, under the interaction of these nanotubes with PSE, the band intensity must decrease, which is observed experimentally.

We note that, after the adsorption of GOX molecules onto SWNT:PSE, the spectral transformation is weaker. For example, the intensities of bands assigned to (7,5), (10,3) and (7,6) nanotubes do not change practically.

3.2.2 Tangential mode

The most intense band in the RR spectra of SWNTs lies in the 1550–1620 cm^{-1} range and corresponds to the high-frequency component of the tangential G mode [20]. This band for nanotubes and their hybrids with PSE and PSE:GOX is shown in Fig. 6. As is seen from Fig. 6, the intense band in the RR spectrum of the nanotubes in bundles (1592.4 cm^{-1}) is low-shifted by 1.7 cm^{-1} in the SWNT:PSE film. This shift takes place, because the interaction energy of nanotubes in bundles decreases due to a weaker nanotube-PSE binding energy. The intense band in the spectrum of the SWNT:PSE:GOX complex has a peak at 1590.5 cm^{-1} , which indicates the insignificant influence of GOX on the RR spectrum of nanotubes:PSE (located at 1590.7 cm^{-1}).

Some differences in the band positions and intensities were obtained after the fitting with the sum of approximation functions. Each experimental spectrum has been fitted with a minimal number of approximation functions (Fig. 6) consisting of the sum of four Lorentzians and one Breit–Wigner–Fano (BWF) function, $I(\omega) = I_0 \{1 + (\omega - \omega_0)/q\Gamma\}^2 / \{1 + [(\omega - \omega_0)/\Gamma]^2\}$ [21], where I_0 , ω_0 , Γ , and q are the intensity, BWF frequency, broadening parameter, and asymmetry parameter, respectively. The BWF function is used for describing the low-frequency spectral band, which appears due to the presence of metallic nanotubes. On the basis of a good coincidence between the experimental spectrum and the sum of approximating curves, the parameters of these curves were determined (Table 2). The total intensity of the whole spectral fragment was set as 100%. As is seen from Table 2, a low-frequency shift from 0.3 to 3.4 cm^{-1}

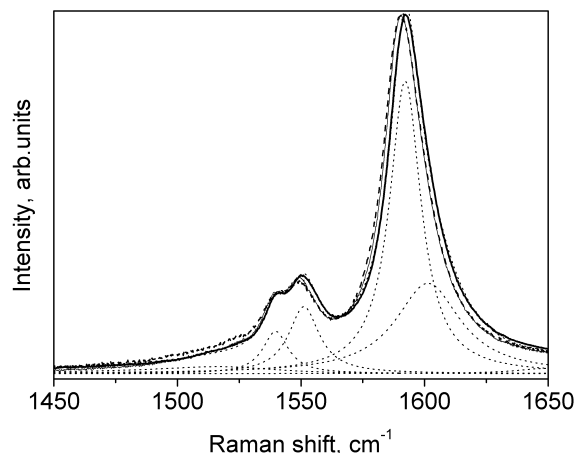


Fig. 6. High-frequency fragment of SWNTs (bold line), SWNT:PSE (thin line), and SWNT:PSE:GOX (broken line) hybrids in the G mode range

range was observed in the film with PSE for all bands of nanotubes.

Thus, in accordance with changes in the RR spectra of nanotubes in the PSE environment relative to the spectrum of pristine nanotubes, we can conclude that the PSE molecule forms a noncovalent hybrid with a carbon nanotube, which favors the further immobilization of enzyme molecules. At the same time, the absence of significant changes in the RR spectrum of the SWNT:PSE:GOX hybrid (as compared with the SWNT:PSE one) evidences that these PSE molecules isolate efficiently the GOX molecules from nanotubes, preventing their direct interaction with the nanotube surface.

3.3. Structure and interaction energy of the SWNT:PSE:GOX complex in the water environment: molecular dynamics modeling

While modeling the SWNT:PSE:GOX complex, we were aimed to reveal whether one PSE molecule is able to keep one GOX molecule (covalently bound to it) near the nanotube surface. The other task was to determine the interaction energies between the PSE:GOX complex and SWNTs. It is known that PSE reacts with amino groups of peptides [8]. In this case, the CO-NH bond is formed. One PSE molecule was attached to one of the lysine side residues of GOX. As a result, a new compound was obtained (denoted as PSE:GOX). It consists of the pyrene fragment and a GOX molecule joined with a linker. The PSE:GOX complex was connected to the SWNT surface by the pyrene fragment at a distance of 3.5 \AA . The system was minimized during 1000 cycles

Table 2. Position (ω_{RBM} , cm^{-1}), width at the half of the height ($\Delta\Gamma$, cm^{-1}), and integral intensities of curves described by Lorentzian and BWF (with the asymmetry parameter $1/q$) functions normalized to the total intensity of the band assigned to G band (S/S_{max})

SWNT				SWNT:PSE				SWNT:PSE:GOX			
ω , cm^{-1}	$\Delta\Gamma$, cm^{-1}	$-1/q$	S/S_G $\times 100\%$	ω , cm^{-1}	$\Delta\Gamma$, cm^{-1}	$-1/q$	S/S_G $\times 100\%$	ω , cm^{-1}	$\Delta\Gamma$, cm^{-1}	$-1/q$	S/S_G $\times 100\%$
1521.7	30.1	0.17	3.1	1520	29.2	0.15	3.9	1518.4	37.8	0.17	5.3
1539.7	12.6		5.7	1539.1	12.2		6.1	1539.4	16.5		8.3
1551.2	15.0		11.1	1550.0	14.6		10.3	1550.5	13.2		7.4
1592.2	15.4		48.8	1590.5	15.1		46.5	1590.0	15.4		45.8
1601.4	31.9		31.3	1598.5	31.4		33.2	1598.0	28.9		33.2

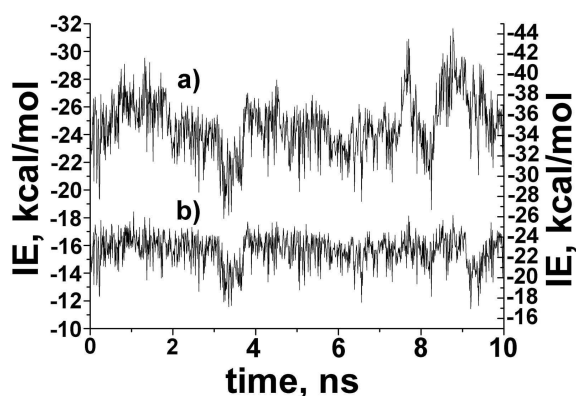


Fig. 7. Interaction energies between PSE and SWNT (a, left scale) and PSE-GOX and SWNT (b, right scale)

and then equilibrated for 10 ns with a 1-fs step. After modeling the total energy of interaction between SWNT and the whole PSE:GOX complex, the interaction energies of SWNT and various parts of this complex were determined. They are shown in Fig. 7. The equilibrated structure of the SWNT:PSE:GOX complex is presented in Fig. 8.

As is seen from Fig. 7, the energy of the interaction between the pyrene fragment and the nanotube surface in the SWNT:PSE:GOX complex (curve a) is in the interval $(-20 - -25)$ kcal/mol. This result agrees very well with the interaction energy between pyrene and nanotubes calculated for the SWNT:PSE complex [14]. Moreover, Fig. 7 demonstrates that, during the whole period of modeling, the pyrene fragment is strongly attached to the nanotube. This evidences that one pyrene “anchor” is able to hold efficiently the GOX enzyme on the nanotube. The total interaction energy between a nanotube and the PSE:GOX complex (Fig. 7, curve b) (from -22 to -27 kcal/mol) is equal to the sum of energies of interactions between PSE and a nanotube, as well as between GOX and a nanotube. Thus, we can determine the energy of interaction between GOX

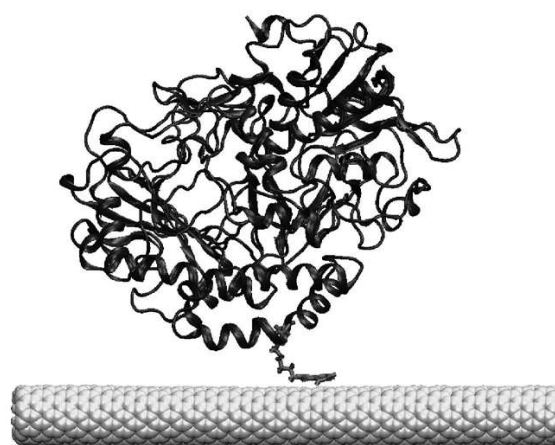


Fig. 8. Equilibrated structure of the SWNT-PSE-GOX complex. Water molecules are not shown

and a nanotube, by subtracting the SWNT:PSE interaction energy from the total interaction energy (Fig. 7, curve b). Thus, the energy of interaction between GOX and a nanotube changes during the modeling from -5 to -2 kcal/mol. This energy is due to the interactions between a nanotube and outward side residues of a GOX molecule. The mutual orientation of GOX and the nanotube surface changes slowly during the modeling. As a result, the GOX–nanotube interaction energy changes as weakly. It may be concluded that the modeling of the SWNT:PSE:GOX complex demonstrates the absence of strong interactions between GOX and the nanotube surface. This fact allows us to suppose that the GOX activity is not changed under the formation of the SWNT:PSE:GOX complex.

3.4. Conductivity of single-walled carbon nanotube networks: effects of environment

We carried out studies of the conductive properties of the single-walled carbon nanotube network sprayed onto a quartz substrate from their solution in dichloroben-

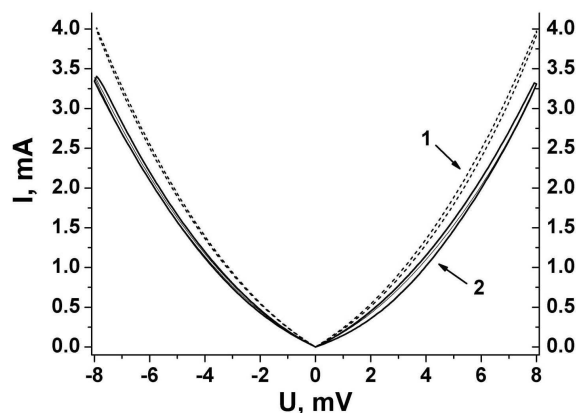


Fig. 9. Current versus voltage for an SWNT network placed between two gold contacts separated by $10\ \mu\text{m}$ gap (curve 1). Curve 2 corresponds to the conductivity of a sample after the adsorption of PSE

zene. The dependence of the current through the carbon nanotube network in the dry state at variations of the voltage (U) between two contacts is shown in Fig. 9 (dotted line). The voltage is changed in $(-8 - +8)$ V range, the maximum current (I) runs up to 4 mA, and the $I(U)$ dependence has nonlinear character. Most likely, the nonlinearity is related to Schottky barriers, which originate at the contact between nanotubes and a gold contact or between nanotubes of different conductivities [22]. In addition, the $I(U)$ dependences manifest a small hysteresis. To avoid the effects of a solution on the volt-ampere characteristics, the presented dependences were obtained in 4–6 days after the fabrication of a nanotube network or after the deposition of biomolecules.

In this study, the effects of bioorganic compounds (PSE and GOX) deposited on the carbon nanotube network on its conductivity have been investigated. After the deposition of the molecular interface (PSE) from methanol and the drying of the film, its conductivity was about 20% less than the initial value (Fig. 9, solid line). Most probably, such a decrease is caused by adsorbed PSE molecules, which induce the appearance of scattering centers for charge carriers on the nanotube surface, as it was observed earlier [2]. It should be noted that the following GOX adsorption (Fig. 9, inside curve 2) has practically no effect on the conductivity of the nanotube network. It is obvious that this molecular interface (PSE) isolates the enzyme from the nanotube surface rather efficiently. The appearance of the hysteresis for the $I(U)$ dependence in similar measurements was explained earlier by the presence of charge traps on the SiO_2 surface. These traps are occupied under the pas-

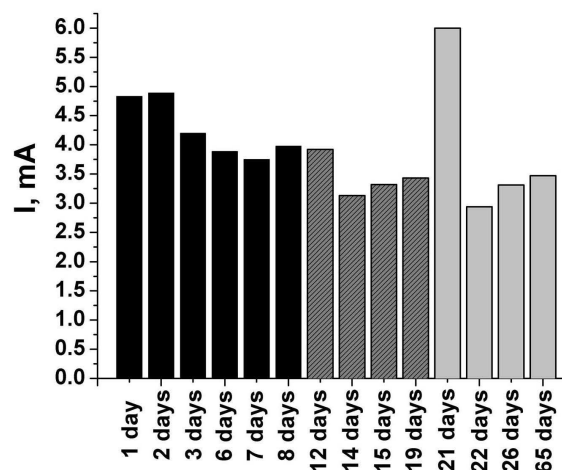


Fig. 10. Time dependence of the maximal current (obtained at 8 V) for a SWNT network placed between two gold contacts separated by $10\ \mu\text{m}$ gap (black column). Dashed and shaded columns correspond to the current through the network measured after the deposition of PSE and the GOX immobilization, respectively

sage of a current in one direction and are not depleted yet, when the current has the opposite direction [19].

In addition, the time dependence was built for the current passing through the nanotube network, beginning from the nanotube network fabrication up to the PSE deposition and the immobilization of GOX (Fig. 10). As is seen from Fig. 10, some spread of current values is observed right away after the nanotube network treatment with a bioorganic substance, which is caused by drying the network after its wetting with methanol or water. After some days, this spread of values becomes narrower. A change in the conductivity is especially noticeable after the treatment of the nanotube network with water. At once after the water evaporation, the film conductivity rises appreciably. Then it reduces in the course of the time, but this takes a rather long time (some days at room temperature).

4. Conclusion

The efficient immobilization of GOX onto a carbon nanotube network through the molecular interface formed by PSE is carried out. This conclusion is based on the analysis of AFM images of the network with the adsorbed enzyme, whose globules locate mainly along a nanotube.

The band corresponding to the high-frequency component of the G mode in the RR spectrum of the nanotube with adsorbed PSE is downshifted by $0.7\ \text{cm}^{-1}$ relative to this band in the spectrum of pristine nan-

otubes. The analysis of the intensities of bands assigned to the RBM of nanotubes with adsorbed PSE in comparison with the spectrum of pristine SWNTs revealed the intensity transformation, which can be explained by a change of the resonance condition with variation of the laser energy. Thus, we concluded that PSE molecules create nanohybrids with SWNTs, which ensures the further enzyme immobilization. As the RR spectrum of an SWNT:PSE:GOX film does not essentially differ from SWNT:PSE ones, this indicates that the molecular interface (PSE) isolates the enzyme from nanotubes strongly enough.

Our studies on the conductive properties of a single-walled carbon nanotube network sprayed onto a quartz substrate from a solution of nanotubes in dichlorobenzene demonstrated that the $I(U)$ dependence has nonlinear character. Most likely, the nonlinearity is related to Schottky barriers, which originate on the contact between nanotubes and the gold electrode, as well as between nanotubes with different conductivities.

The deposition of bioorganic compounds (PSE and GOX) on the carbon nanotube network is accompanied by a decrease of their conductivity. Most probably, such a decrease is caused by adsorbed PSE molecules, which induce the appearance of scattering centers for charge carriers on the nanotube surface. The following GOX adsorption has practically no effect on the conductivity of the nanotube network that evidences the reliable isolation of the nanotube surface from the enzyme by means of the molecular interface (PSE). While studying the properties of carbon nanotube networks, whose surface underwent the treatment with a solution, it is necessary to consider the gradual desorption of a solvent from the nanotube surface (especially, this concerns water).

The authors acknowledge the Computational Center at B. Verkin Institute for Low Temperature Physics and Engineering of the National Academy of Sciences of Ukraine.

1. K. Balasubramanian and M. Burghard, *Anal. Bioanal. Chem.* **385**, 452 (2006).
2. G. Gruner, *Anal. Bioanal. Chem.* **384**, 322 (2006).
3. S. Roy and Z. Gao, *Nano Today* **4**, 318 (2009).
4. K. Besteman, J.O. Lee, F.G. Wiertz, H.A. Heering, and C. Dekker, *Nano Lett.* **3**, 727 (2003).
5. X. Dong, C.M. Lau, A. Lohani, S.G. Mhaisalkar, J. Kasim, Z. Shen, X. Ho, J.A. Rogers, and L.-J. Li, *Adv. Mater.* **20**, 2389 (2008).
6. P.W. Barone, S. Baik, D.A. Heller, and M.S. Strano, *Nature Mater.* **4**, 86 (2005).
7. S.S. Karajanagi, A.A. Vertegel, R.S. Kane, and J.S. Dordick, *Langmuir* **20**, 11594 (2004).
8. R.J. Chen, Y. Zhang, D. Wang, and H. Dai, *J. Am. Chem. Soc.* **123**, 3838 (2001).
9. S.G. Stepanian, V.A. Karachevtsev, A.Yu. Glamazda, U. Dettlaff-Weglikowska, and L. Adamowicz, *Mol. Phys.* **101**, 2609 (2003).
10. W.E. Alvarez, F. Pompeo, J.E. Herrera, L. Balzano, and D.E. Resasco, *Chem. Mater.* **14**, 1853 (2002).
11. C.P. James, B. Rosemary, W. Wang, J. Gumbart, E. Tajkhorshid, E. Villa, C. Chipot, R.D. Skeel, L. Kale, and K. Schulten, *J. Comput. Chem.* **26**, 1781 (2005).
12. A.D. MacKerell jr., D. Bashford, M. Bellott, R.L. Dunbrack jr., J.D. Evanseck, M.J. Field, S. Fischer, J. Gao, H. Guo, S. Ha, D. Joseph-McCarthy, L. Kuchnir, K. Kuczera, F.T.K. Lau, C. Mattos, S. Michnick, T. Ngo, D.T. Nguyen, B. Prodhom, W.E. Reiher, B. Roux, M. Schlenkrich, J.C. Smith, R. Stote, J. Straub, M. Watanabe, J. Wiorcikiewicz-Kuczera, D. Yin, and M. Karplus, *J. Phys. Chem. B* **102**, 3586 (1998).
13. G. Wohlfahrt, S. Witt, J. Hendle, D. Schomburg, H.M. Kalisz, and H.-J. Hecht, *Acta Cryst. D* **55**, 969 (1999).
14. V.A. Karachevtsev, S.G. Stepanian, A.Yu. Glamazda, M.V. Karachevtsev, V.V. Eremenko, O.S. Lytvyn, and L. Adamowicz, *J. Phys. Chem. C* **115**, 21072 (2011).
15. W. Humphrey, A. Dalke, and K. Schulten, *J. Molec. Graphics* **14**, 33 (1996).
16. S.G. Stepanian, M.V. Karachevtsev, A.Yu. Glamazda, V.A. Karachevtsev, and L. Adamowicz, *J. Phys. Chem. A* **113**, 3621 (2009).
17. C. Fantini, A. Jorio, A.P. Santos, V.S.T. Peressinotto, and M.A. Pimenta, *Chem. Phys. Lett.* **439**, 138 (2007).
18. S.K. Doorn, *J. Nanosci. Nanotech.* **5**, 1023 (2005).
19. S.G. Chou, H.B. Ribeiro, E.B. Barros, A.P. Santos, D. Nezich, Ge.G. Samsonidze, C. Fantini, M.A. Pimenta, A. Jorio, F. Plentz Filho, M.S. Dresselhaus, G. Dresselhaus, R. Saito, M. Zheng, G.B. Onoa, E.D. Semke, A.K. Swan, M.S. Ünlü, and B.B. Goldberg, *Chem. Phys. Lett.* **397**, 296 (2004).
20. M.S. Dresselhaus and P.C. Eklund, *Adv. Phys.* **49**, 705 (2000).
21. A.M. Rao, P.C. Eklund, S. Bandow, A. Thess, and R.E. Smalley, *Nature* **388**, 257 (1997).
22. S. Heinze, J. Tersoff, R. Martel, V. Derycke, J. Appenzeller, and P. Avouris, *Phys. Rev. Lett.* **89**, 106801 (2002).
23. W. Kim, A. Javey, O. Vermesh, Q. Wang, and H. Dai, *Nano Lett.* **3**, 193 (2003).

Received 12.12.11

ІММОБІЛІЗАЦІЯ ГЛЮКОЗООКСИДАЗИ НА СІТКУ
ОДНОСТІННИХ ВУГЛЕЦЕВИХ НАНОТРУБОК

*В.О. Карачевцев, О.Ю. Гламазда, Є.С. Заруднев,
М.В. Карачевцев, В.С. Леонт'єв, О.С. Літчик,
О.С. Литвин, О.М. Плохотниченко, С.Г. Степан'ян*

Резюме

При створенні біологічних сенсорів з використанням одностінних вуглецевих нанотрубок (ОВНТ) треба вирішити таку важливу проблему, як іммобілізація молекули, яка повинна розпізнати мішень, на поверхні нанотрубок. В даній роботі проведена іммобілізація ферменту глюкозооксидаза (ГОК) на поверхню сітки нанотрубок, яка була одержана шляхом осадження нанотрубок з їх розчину у діхлорбензолі за допомогою спреї-методу. У ролі молекулярного інтерфейсу було застосовано сукцинімідний ефір 1-піренбутанової кислоти (ПСЕ), біфункціональна молекула якого забезпечує хімічний зв'язок з оболонкою ферменту, а друга її частина (піренова) адсорбується на поверхню нанотрубки. Використання такого молекулярного інтерфейсу виключає, з одного боку, пряму адсорбцію

ферменту на поверхню нанотрубки, яка знижує його активність, а з другого, забезпечує локалізацію ферменту поблизу нанотрубки. Порівняння спектрів резонансного комбінаційного розсіювання світла (РКРС) нанотрубок з їх спектром в оточенні ПСЕ вказує на створення наногібриду молекулою ПСЕ з нанотрубкою, що дає підставу для подальшої іммобілізації ферментів. Оскільки спектри РКРС плівок ОВНТ:ПСЕ:ГОК суттєво не відрізняються від спектрів ОВНТ:ПСЕ, то можна стверджувати, що молекулярний інтерфейс ПСЕ достатньо міцно ізолює фермент від нанотрубки. Ефективна іммобілізація ферменту ГОК поблизу вуглецевої нанотрубки завдяки ПСЕ підтверджується за допомогою зображень, отриманих атомно-силовим мікроскопом. Молекулярна динаміка дозволила встановити структури отриманих нанобіогібридів та енергії міжмолекулярної взаємодії між компонентами потрібного комплексу у водному оточенні. Було також досліджено провідні властивості сітки ОВНТ з адсорбованими молекулами ПСЕ та ГОК. Адсорбція молекул ПСЕ на сітку з ОВНТ супроводжується зменшенням провідності, яке, скоріш за все, пов'язано з появою розсіювальних центрів для носіїв заряду у нанотрубках.